Transactions of the Japan Welding Society, Vol. 24, No. 2, October 1993

Investigation on Solidification Process by Fracture Surface Observation of Aluminum Alloy Welds Specimen Broken by High Speed Breaking Test*

By Shozaburo OHTA** and Kimioku ASAI**

Abstract

Behavior of TIG arc spot welds of an Al alloy A5083 thin plate during cooling and solidification process was investigated by the following methods. Temperature of welds was measured during heating and cooling process by using very slender thermocouples. Weld specimen was broken any time during cooling and solidification process by using a high speed breaking apparatus. Afterwards, morphological macro-and micro-structures of fracture surface were observed using the electron microscope. The results obtained are as follows:
1) *There developed a liquefied grain boundary, which is called a brittle zone, and a partial liquefied grain boundary, which is called a low ductility zone, in HAZ when some time elapsed after arc stop.*
2) *Solidification end was determind by confirming disappearance of liquid phase on fracture surface. As a result, it was found that the temperature of solidification end weld metal was considerabl lower* (440~425 °C) *than solidus temperature* (579 °C) *of base metal.*
3) *CCSP diagram was obtained from fractography analysis by determining solidification end, which was difficult to determine from analysis of cooling and solidification curve.*

Key Words: *Solidification process, Fracture surface, Al alloy, Temperature measurement, Solidification end, Solidification temperature range, Low ductility zone, Highspeed breaking test, Brittle zone, Fractography,*

1. Introduction

Hot cracking is one of the most serious defects which occur in the weld joints of aluminum alloys and many researches have been focussed on this subject[1)-23)]. Few researches appear, however, to be based on a full understanding of the cooling and solidification process of the welded joint. Thus we are working for the purpose of fully clarifying such process and thereby the origination and development of hot cracks in a welded joint, and, based on that, evaluation of the sensibility to hot cracking of the material.

Our first step was analysis by temperature measurement of the solidification behavior of both aluminum metal and alloy after arc welding, quantitatively and over time, and as a result, we could determine by now the temperature distribution in molten pools, cooling rates of the weld metal, solidification rates (that is progress of solidification front), solid fraction increase relative to liquid within the coexisting zone, etc. We could also get a general idea of the whole cooling and solidification process by means of the CCSP (Continuous Cooling and Solidification Process) diagrams which indicated those process parameters as functions of time or position[24)-26)].

It became also apparent that we cannot tell exactly when the solidification has completed simply by analysis of solidification curves based upon temperature measurements, because the curves generally show a monotonous descent without any characteristic discontinuity for the later stage when the latent heat emission gradually decreases. However, understanding the later stage, where liquid film may still remain along grain boundaries, and detecting, rather than the initiation, the completion of the solidification process, where the film has wholly disappeared, are more important for the purpose of understanding the origination and development of hot cracking and thus evaluating the sensibility to hot cracking.

Therefore, we tore rapidly weld specimens and examined the fracture structure under electron microscope at several points of time during the solidification process, while measuring the temperature of the specimens. We could thereby observe the variation with time and, especially, the complete disappearance of the remaining volume of liquid film in the grain boundaries (that is completion of the solidification), and relate it to the temperature measured. The results are also represented in an CCSP diagram as in our previous work[26)].

2. Sample Material and Experimental Method

The sample material we used was a 1 mm thick (JIS) A5083 Aℓ-Mg alloy sheet, as in the previous work[26)]. The chemical composition is shown in Table 1. It was cut into 140 by 80 mm rectangular specimens, with the length set in the direction of rolling. They were spot welded in the center with a TIG arc (DCEP) at welding

* Received: 1 August, 1993
** Member, Musashi Institute of Technology, 1-28-1 Tamazutsumi, Setagaya-ku, Tokyo, 158 Japan

current of 40 A, arc voltage of 20 V, and arc duration of 10 s. The temperature of the welds was measured as described in our earlier works[24),25)].

In order to rapidly tear specimens we devised a horizontal stretching machine, which used a pneumatically actuated hydraulic system. Pressure was produced by compressed air, boosted and converted to a hydraulic pressure, which was transmitted to the cylinder, via a magnet valve and a flow control valve, and drove the piston to stretch the specimen until the latter was torn down. This machine was capable of stretching the specimen at an average rate of 400 to 650 mm/s with the maximum stroke of 20 mm, at any point of time with precision to 1/100 s during the solidification process. Samples were taken and broken at an interval of 1/10 s from the time the arc was turned off, and the fractures were examined under electron microscope to observe the variation of the remaining liquid in the grain boundaries during the cooling solidification process. We paid special attention to complete disappearance of the liquid film from the fracture surface at the last stage of solidification, for which we used as an indication the general dimpling of the broken surface.

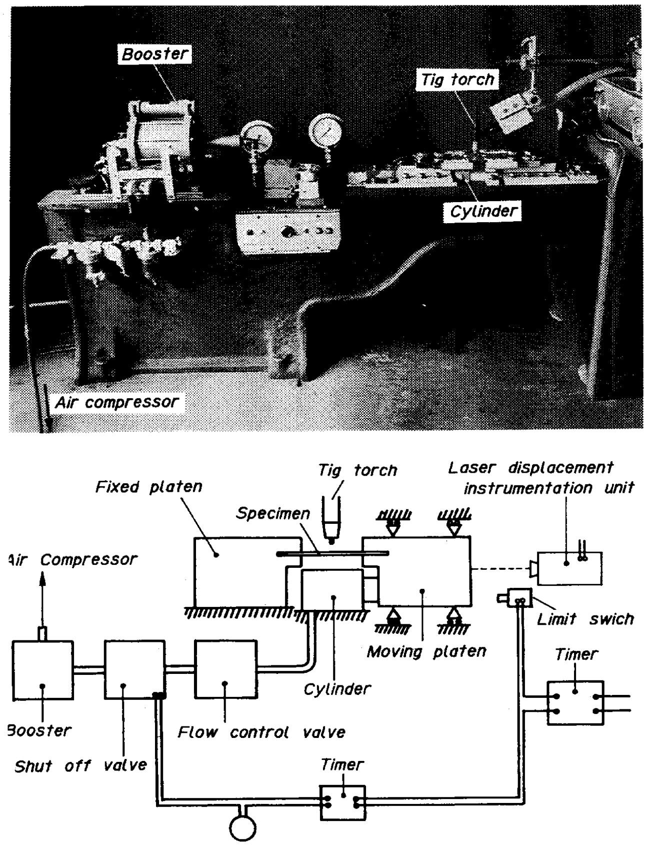

Fig. 1 Appearance and operating principle of a high speed breakihg machine.

Table 1 Chemical compositions of a material used.

Al-alloy (t=1mm)	Chemical compositions (wt%)								
	Cu	Si	Fe	Mg	Mn	Cr	Zr	Ti	Zn
A5083	0.02	0.14	0.24	4.59	0.62	0.11	0.01	0.01	--

3. Results and Discussions

3.1 *Preparation of CCSP diagram*

Fig. 2 (a) shows some thermal cycle curves for the cooling half obtained by temperature measurement in this work, and (b) shows the specimen geometry with the placement of the thermocouples. The curves were analyzed as in earlier works[24)–26)] and represented in an CCSP diagram to show the positions of the weld relative to the fusion boundary (F.B.) as a function of the time counting after the arc extinguishment, along with the temperature and any phase change (Fig. 3). In this diagram, the curves —○— trace the varying position of equilibrium solidification (635 °C) and —●—, that of the solidification front (S.F.). The curve —▲— represents grain boundaries on the weld metal side, which progressed in the solidifi-cation process, and —★—, the dendritic region boundaries over which a characteristic change was observed in transition from unsolidified to solidified phase. The —△— and —☆— curves refer to the corresponding boundaries on the heat affected zone (HAZ) side. Those curves, which will be explained in particular in the following paragraphs, and others divide the diagram of Fig. 3 into the regions from (I) to (VII), which may be briefly summarized as: (I) completely liquid, (II) and (III) solid-liquid coexisting, where both the grain and dendritic region

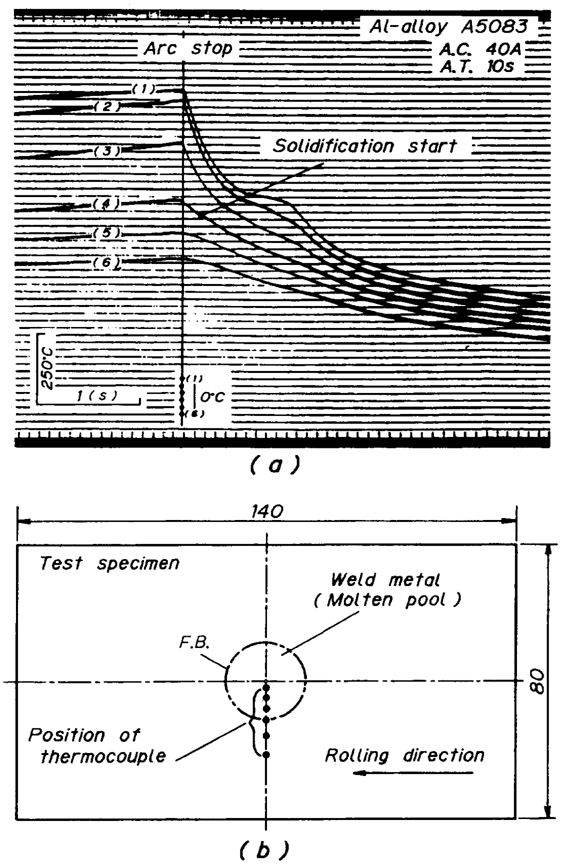

Fig. 2 Shape and dimensions of a test specimen and an example of cooling curve obtained by temperature measurement.

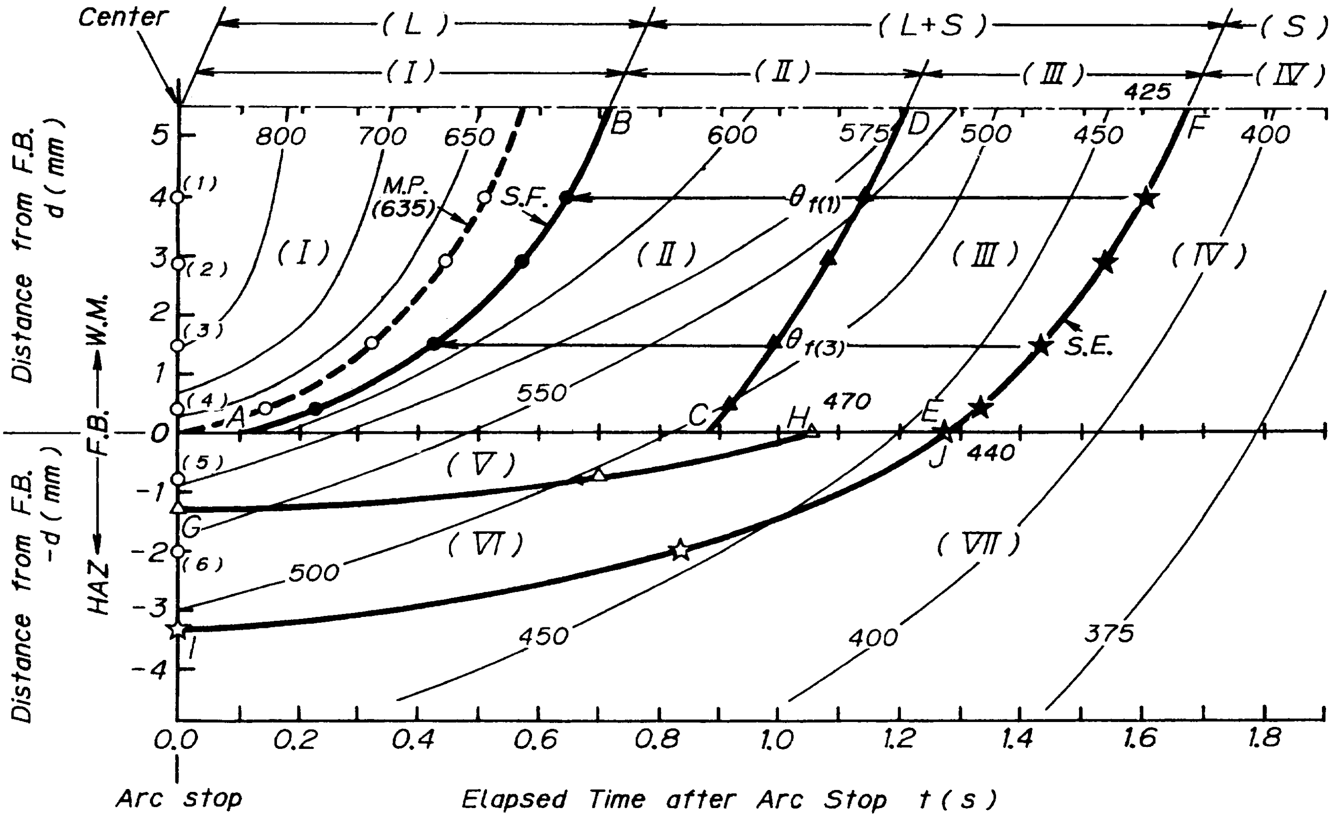

Fig. 3 Continuous Cooling Solidiffication Process (CCSP) diagram for Al alloy A5083 TIG arc spot weld.

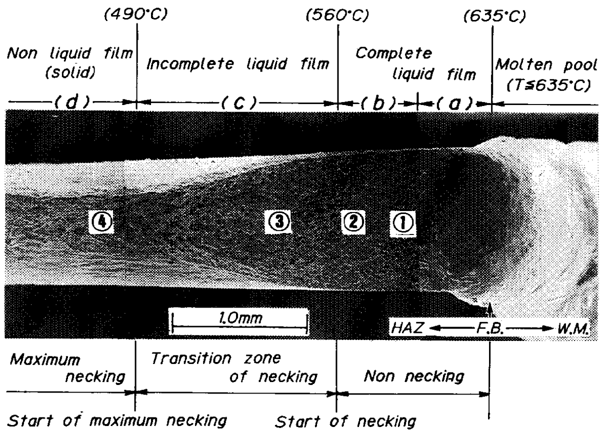

Fig. 4 Electron micrograph (SEM) of fracture surface of HAZ broken just after arc stop.

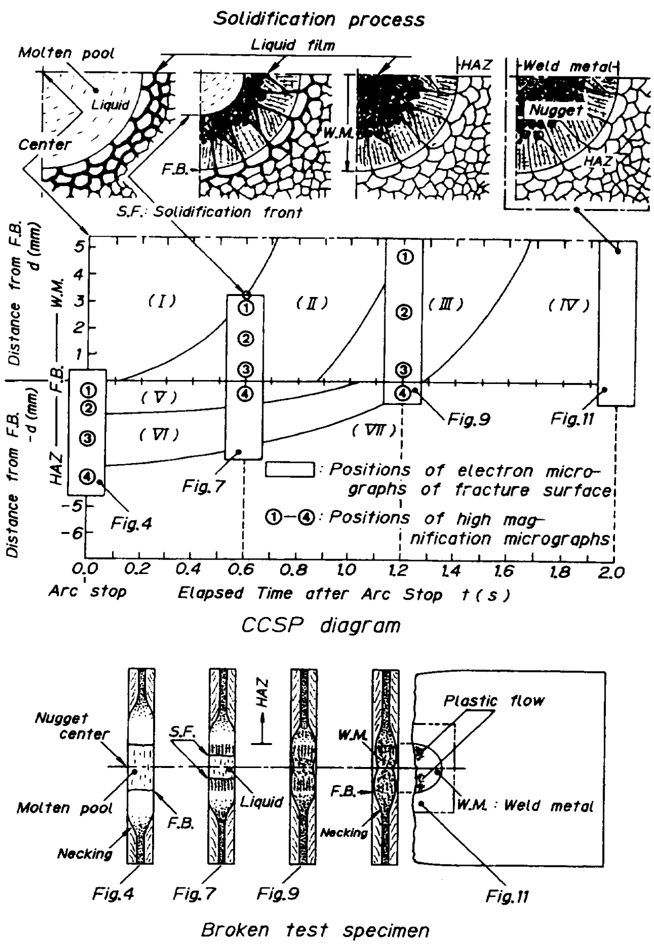

Fig. 5 Positions of electron micrographs in Figs. 4-11 on CCSP diagram.

boundaries are covered with liquid totally (II); or partly to appear local solid-solid contacts or junctions; this increased with time relative to the liquid film area which decreased accordingly (III); (IV) designates the region where the solidification has completed, leaving no liquid film in either boundaries. On the HAZ side, the grain boundaries were (V) totally covered, (VI) partly liquefied, or totally solidified (VII).

3.2 *Fracture structures after arc extinguishment*

Fig. 4 shows the scanning electron micrographic (SEM) image at a low magnification (×50) of a specimen broken at t=0.0 s (that is immediately after the arc had been turned off), to which the time counting was related. Fig. 6 relates on an CCSP diagram the weld positions ①-④ which correspond to the structure

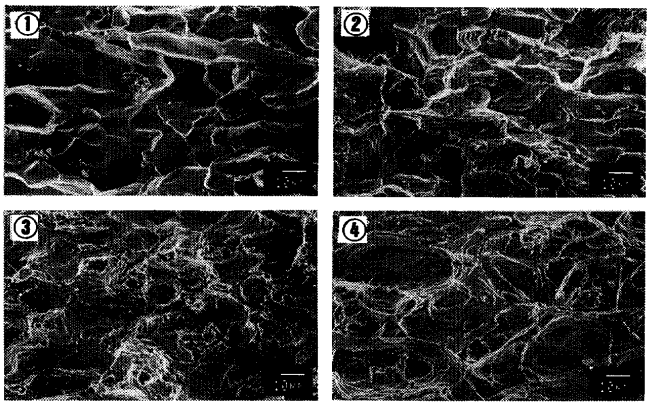

Fig. 6 High magnification micrographs (SEM) at positions ① ~④ in Fig. 4.

types ①-④ of the SEM image in Fig. 4, to the time points when the samples were taken. Solid phase had not formed in the molten pool at the stage of Fig. 4, and the fractured structure was observed only in the HAZ side. A fractured sturucture was observed only in the HAZ side. The divisions (a) and (b) were places where little compression formed on the specimen when stretch-broken, with the grain boundaries totallyliquefied (so-called brittleness region). They extended over the F.B. to a distance of about 1.25 mm, and corresponded to the region (V) in Fig. 3. The division (a) is the HAZ portion which could not be observed because liquid flowed in and covered the surface when the specimen was broken. The division (c), corresponding to (VI), is a transitional area between (b) and (d) where grain boundaries were partly liquefied and the ductility decreased. Those are the three divisionsto make up macroscopically the fracture surface HAZ portion. The temperature measurements at division interfaces were done as shown in Fig. 3: 560 °C for (b)/(c), or (V)/(VI), and 490 °C for (c)/(d) or (VI)/(VII), approximately. The length of the portion where the grain boundaries were either totally or partly liquefied, was about 3.3 mm as taken between the F.B. and the 490 °C point. Figs. 6 ① to ④ show again the SEM images of Fig. 4 but with a higher magnification (×1000). As the images show, the fracture surface was totally covered by liquid film at ①, and its thickness apparently decreased gradually toward ②. At ③ an early stage of dimpling was observed along with boundaries covered partly with liquid. At ④ the fracture showed a general dimpling. Thus it is concluded that the presence of liquid film along the grain boundaries may cause the brittleness of the zones (a) and (b) in Fig. 4, which shows a brittleness fracture with little compression.

The temperature at which the liquid film has disappeared is about 490 °C at the (c)/(d) interface, as shown above in Fig. 4. This is significantly lower than the solidus point for A5083, which is nominally 579 °C[27]. This may be probably due to these two effects combined: first, the lowering of the equilibrium solidus point itself which is caused by enrichment of the solute in grain boundaries, and, second, the supercooling which may occur at such high cooling rates in the weld — far higher than in more common foundry — and which may lead to lower equilibrium solidification and eutectic points, as often well seen at such cooling rates[28)-31)].

3.3 *Fracture structures during the solidification process*

3.3.1 Earlier stage of solidification

Fig. 7 shows the SEM image at a lower magnification of the fractured face of the specimen broken at t= 0.6 s, as well as an oblique view showing the top face (see also Fig. 5). By this time, much solid has formed in the molten pool with the solidification front (S.F.) arriving at about 60 % of the pool radius. Thus in this case the positions were closer to the F.B. than in the case shown in Fig. 4 where the compression on the HAZ side originated or reached the maximum. In the weld metal, the macroscopic fracture images show solidified structures which gradually change from mostly columnar to equiaxial grains, when taken from F.B. to molten pool center, via a transitional zone with their coexistence between them.

The structures at ① to ④ in this figure are also shown in Fig. 8 at a higher magnification (×1000) (see

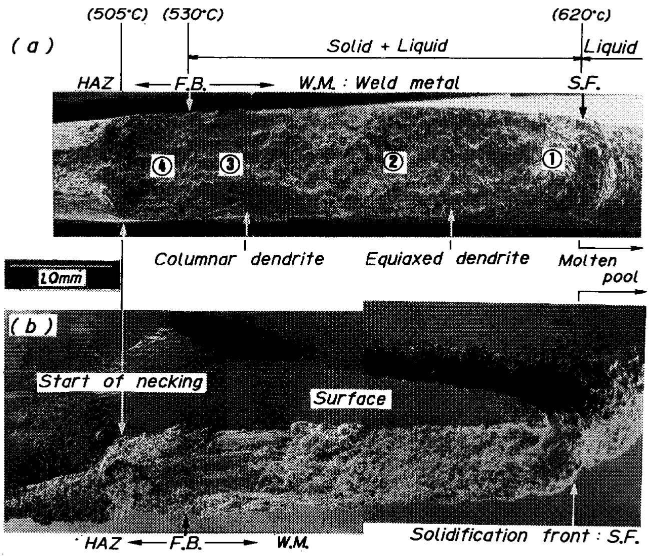

Fig. 7 Fracture surface and its bird's-eye view (SEM) of a specimen broken at 0. 6 s after arc stop.

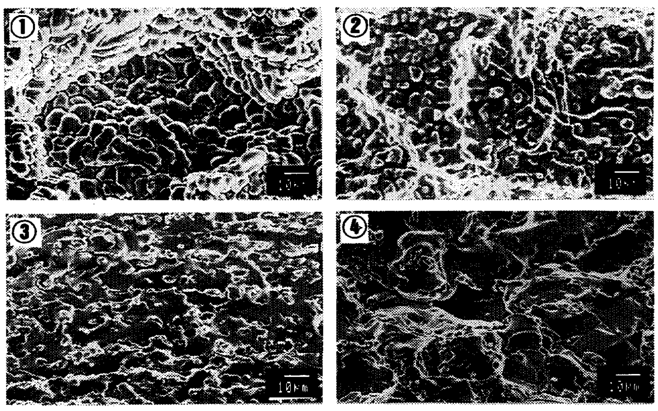

Fig. 8 High magnification micrographs (SEM) at positions ① ~④ in Fig. 6.

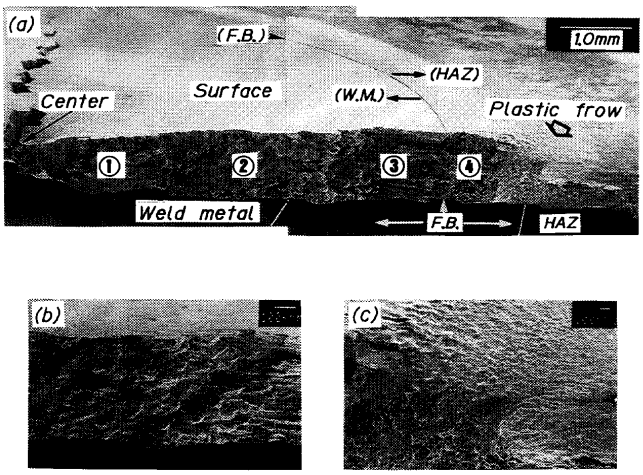

Fig. 9 Bird's-eye view and a partially magnified micrograph (SEM) of fracture surface broken at 1. 2 s after arc stop.

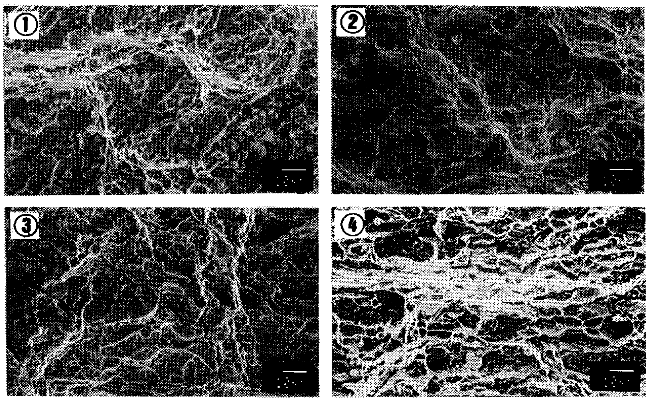

Fig. 10 High magnification micrograph (SEM) at positions ① ~④ in Fig. 8.

also Fig. 5). Although they may give different impressions due to the different solidified structures, it is apparent that each surface is covered totally by liquid film. The liquid still appears to flow to some extent along the grain boundaries. It may thus be considered that no portion of the weld metal did have any effective resistance to fracture at this stage of solidification.

3.3.2 Later stage of solidification

Fig. 9 shows an oblique panoramic view of the whole fracture (a), as well as details of a part of the specimen fractured at t=1.2 s (b) and (c) (see also Fig. 5). In this case the surface exhibits a plastic flow in the HAZ very close to the F.B. and a compressed fracture face, so it is evident that the base metal has recovered ductility outside the F.B.. SEM images taken at ① to ④ in Fig. 9 at a higher magnification will be seen in Fig. 10 (see also Fig. 5). The zone ①, close to the center of the weld metal, shows much liquid film, but there are also parts with a noticeable dimple formation at an early stage with weak bonding. Such parts increase the fracture and form a clearer dimple in a zone as pey approach to the F.B., clearer in ③ than in ②; and around ④, the fracture is almost full of dimples. Thus it may be considered that 1.2 s after the arc extinguishment, the liquid film has almost disappeared

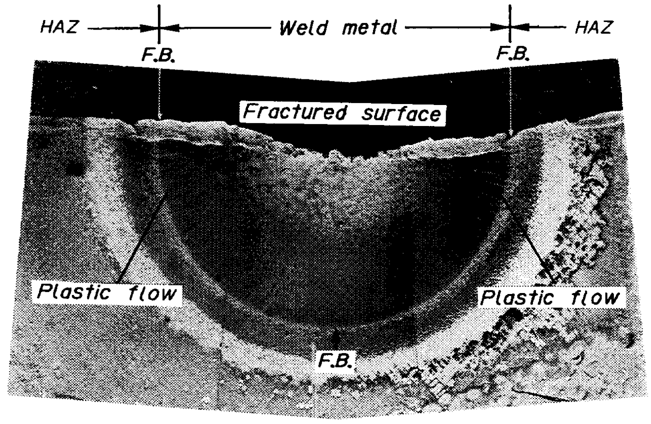

Fig. 11 Plastic flow observed on weld surface of the specimen broken at 2. 0 s after arc stop.

around the F.B. and also in the HAZ, at the last stage of the solidification process.

3.4 *Fracture structures after complete solidification*

The structure shows a general dimpling when fractured after the solidification has completed and the liquid film has totally disappeared. Our experiment results showed that it completed in about 1.7 s after the arc was turned off. Fig. 11 shows as an example the macroscopic image of a specimen broken at 2.0 s after the arc extinguishment, where the solidification has completed (see also Fig. 5). It is apparent that the ductility has reached its maximum with a macroscopically noticeable plastic flow in the surface layer close to the fractured surface, although a slight recess is observed in the center.

In the development illustrated above of fracture structure with time following the arc extinguishment (t=0.0 s) at different positions in the specimens on both the weld and HAZ sides, the curve CD (—▲—) in CCSP diagram of Fig. 3, traces the positions which indicate the earliest sign of dimpling and which correspond to the temperature range between about 490° around the F.B. and about 575 °C at the center of the molten pool. The curve EF (—★—) traces the limits where the liquid film has completely disappeared from the grain boundaries in the solid-liquid coexistence, and where a general dimpling occurs, with the temperature range from 440 °C around the F.B. to 425 °C, approx. at the center of the molten pool. This is the curve which represents the complete solidification and the maximum ductility. The temperatures that all those curves point at the end do not depend on the direction of rolling of the base metal.

The temperatures we obtained for the complete solidification of the weld metal were even lower than the equilibrium eutectic point of 450 °C in our sample material which was basically an A5083 Aℓ-Mg binary alloy. The weld metal cooled at high rates and thus underwent a non-equilibrium solidification, so it was possible that the diffusion of solute is significantly limited during the solidification and eventually its concentration in the liquid may rise considerably in grain boundaries. If the concentration reaches the

Table 2 Explanation of classified area on CCSP diagram.

Position	Mark	Area on CCSP diagram	Phase	Fractured Surface
Weld Metal (W.M.)	I	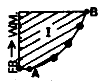	Liquid	–
	II	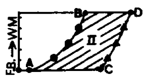	L+S	Liquid Film
	III	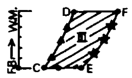	L+S	Liquid Film + Dimple
	IV	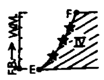	Solid	All Dimple
HAZ	V		L+S	Liquid Film on Grain Boundary
	VI		L+S	Liquid Film + Dimple
	VII	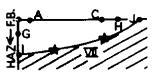	Solid	All Dimple

eutectic level, the solution will have the equilibrium eutectic point as the solidus temperature. Given that eutectic temperatures can be lowered when supercooled at high cooling rates[29)–31)], and tend to be more so than equilibrium solidification temperatures[29)], it seems that it is because the cooling rates we used were too high when passing the eutectic point (450 °C) of the binary system that our solidification completion temperatures fell below this temperature. Also the difference in such temperatures as about 440° and 425 °C around the F.B. and in the center of the weld metal, respectively, may be due to the difference in cooling rates: 140-150 and 220-230 °C/s, respectively, beyond the equilibrium eutectic temperature.

Regarding the HAZ, the curve GH (—△—) traces the limits where the macroscopic compression has just become noticeable in the fracture; so in the zone closer to the F.B., there was no appreciable compression, while the surface was totally covered by liquid film. The temperature ranged from 560 °C at the point G to 470 °C, approximately, at H. The curve IJ (—☆—) traces the limits where the compression has just reached the maximum; so this, just like the curve EF for the weld metal side, represents the maximum ductility. The temperature varied from 490 °C at the I to 440 °C, approximately, at J. The reason set forth under section 3.2 may be also applicable to the observation that the curve IJ lies significantly below the nominal solidus of the A5083. Thus the solution enrichment in grain boundaries appears to be an important factor in the (study of) solidification process. However there are so far very few observations of this behavior conducted quantitatively or as a function of time, and further discussions will be necessary on this subject based on experimental results to come.

The curves IJ and EF meet each other on the F.B. at about 1.3 s (after the arc extinguishment). It is thus apparent that the ductility of the HAZ reached its maximum in 1.3 s, or at temperatures fell below 440 °C.

As shown in Fig. 3, the CCSP diagram is divided by the curves AB, CD, EF, GH and IJ, into the regions (I) to (VII). Table 2 summarizes the phases and structural characteristics observed in the regions.

4. Conclusions

Specimens of A5083 Aℓ-Mg alloy sheet were spot welded by TIG arc, and then subjected to a rapid fracture test at points of time in the cooling solidification process after the welding was terminated. The process was discussed based on the scanning electron microscopy and temperature measurements, with the conclusions as follows:

1) The HAZ has, for a certain period after the arc extinguishment, both so-called brittleness region, caused by grain boundary general liquefaction, and so-called ductility reduced region caused by partial liquefaction. The liquid film gradually reduces in volume with time, or with temperature decrease, until it totally disappears at an F.B. temperature of about 440 °C, when the HAZ exhibits the highest ductility in the process accordingly.
2) The grain boundaries within the liquid/solid coexisting region are totally covered by liquid film down to a certain temperature, which may be about 490 °C around the F.B. or 575 °C in the weld metal center. The liquid film gradually decreases with time. Taking the loss of the liquid film as the completion of solidification, the temperature for such loss is 440 °C around the F.B. and about 425 °C in the weld metal center, which are both significantly lower than the nominal solidus temperature of A5083 at 579 °C. Those values are independent of the direction of rolling of the base metal.
3) The analysis of the fracture faces makes it possible to establish the completion of the solidification process, which is very difficult by that of the cooling/solidification process based on temperature measurement alone. This leads to the development of CCSP diagram which particularly indicates the phase variation with time and with position in the whole cooling and solidification process.

References

1) W. I. Pumphrey and J. V. Lyons: "Cracking During the Casting and Welding of the More Common Binary Aluminum Alloy", J. Inst. Metals, Vol. 74, No. 488 (1-4), (1948), 439～455.
2) J. D. Dowd: "Cracking of Alumimum Alloy, W. J., Vol. 31. No. 10, (1952), P. 448s-456s.
3) J. C. Borland: Generalized Theory of Super-Solidus Cracking in Welds (and Casting), British W. J., Vol. 7, No. 8 (1960), P. 508s-512s

4) J. C. Borland, J. H. Rogerson: Examination of the Patch Test for Assessing Hot Cracking Tendencies of Weld Metal. British W. J. Vol. 9, No. 8, (1962), P. 494s-499s5)
5) J. H. Dudas and F. R. Collins: "Preventing Weld Crack in High-Strength AlumimumAlloys", W. J., Vol. 45, No. 6 (1966) P. 241s-249s
6) F. E. Gibbs: "Development of Filler Metals for Welding Al-Zn-Mg Alloy 7039, Weldment Tencil Tests and a Multipass Upon in Developing a Strong Crack-Resistant Filler Metal Alloy", W. J., No. 10 (1966) P. 445s-453s
7) S. Sugiyama and T. Fukui: "Study on Weldable Al-Zn-Mg Alloy (Report 2)", J. JWS, Vol. 35, No. 11 (1966) P. 1122-1129 (in Japanese)
8) S. Sugiyama and T. Fukui: "Study on Weldable Al-Zn-Mg Alloy (Report 3)", J. JWW, Vol. 36, No. 11 (1967) P. 1194-1202 (in Japanese)
9) T. Fukui: "Study on Eutectic-Melting and Micro-Fissuring of Welds in Aluminum Alloy", J. JWS, Vol. 38, No. 6 (1969) P. 20-29 (in Japanese)
10) J. Hernaer and A. Madeoner: "Investigation of Hot Tearing in Al-Zn-Mg Alloy, W. J., Vol. 51, No. 6 (1972) P. 281s-294s
11) T. Senda, F. Matsuda and G. Takano: "Studies on Solidification Crack Susceptibility for Weld Metal with Trans-Varestraint Test (2)", Journal of the Japan Welding Society, Vol. 42, No. 1 (1973) P. 48-56. (in Japanese)
12) K. Ando, S. Nakata, K. Kisida and Y. Tohei: "Hot Deformability of Weld Metal", Journal of the Japan Welding Society", Vol. 42, No. 8 (1973) P. 22-31 (in Japanese)
13) K. Ando, S. Nakata, K. Kisida and Y. Tohei: "Occurring and Developing Mechanism of Transverse Hot Cracking due to Rotation Deformation of Specimen and the Method of Assessment of Hot Cracking Suseptibility, Including Criticism of on Houldcroft Hot Cracking Test", J. JWS, Vol. 42, No. 9 (1973) P. 37-47. (in Japanese)
14) Y. Arata, F. Matsuda, K. Nakata and I. Sakaki: "Solidification Crack Susceptibility of Aluminum Alloy Weld Metal (Report 1)-Characteristics of Ductility Curves during Solidification by Means of the Trans-Varestraint Test", Trans. JWRI, Vol. 5, No. 2 (1977) P. 53-67. (in Japanese)
15) H. H. Tamura, N. Kato, S. Ochiai and Y. Katagiri: "Cracking Study of Aluminum Alloy by the Variable Strain Hot Cracking Test", Trans. JWS, Vol. 8, No. 2 (1977) P. 143-149. (in Japanese)
16) F. Matsuda, K. Nakagawa and S. Harada: "Moving Characteristics of weld Edges during Solidification in Relation to Solidification Cracking in GTA Weld of Aluminum Alloy Thin Sheet", Trans. JWRI, Vol. 9, No. 2 (1980) P. 83-93. (in Japanese)
17) F. Matsuda, K. Nakata, K. Ari and K. Tsukamoto: "Comparison of Weld Crack Susceptibility of Recent Aluminum Alloys", Trans. JWRI, Vol. 10, No. 1 (1981) P. 71-79. (in Japanese)
18) F. Matsuda, K. Nakata, K. Tukamoto and Uchiyama: "Effect of Additional Element on Weld Solidification Crack Susceptibility of Al-Zn-Mg Alloy (ReportIII), Trans. JWRI, Vol. 13, No. 1 (1984) P. 57-66. (in Japanese)
19) I. E. Hernandey and T. H. North: "The Influence of External Local Heating in Preventing Cracking During Welding of Aluminum Alloy Sheet", W. J., Vol. 63, No. 3 (1984) P. 84s-90s
20) F. Matsuda, H. Nakagawa, S. Tomita and K. Sorada: "Behaviors of Solidification Front, Initiation and Propagation of Solidification Crack", Guarterly J. JWS, Vol. 6, No. 3, (1988) P. 82-88 (in Japanese)
21) F. Matsuda, H. Nakagawa, S. Tomita, H. Tamoto and Y. Honda: "Measuring of Critical Strain for Initiation of Solidification Crack by Rapid Tenaile Cracking Test", Quarterly J. JWS, Vol. 6, No. 3 (1988) P. 89-93 (in Japanese)
22) F. Matsuda, K. Nakata, Y. Nishio, K. Tsukamoto and S. Johgan: "Effect of Zirconium Addition on Improvement of Solidification of Al-Zn-Mg Alloy Weld", Quarterly Journal of the J. W. S., Vol. 4, No. 1 (1986) P. 115-120. (in Japanese)
23) F. Matsuda, K. Nakata, K. Tukamoto and S. Johgan: "Effect of Electromagnetic Stirring on Improvement of Solidification Crack Susceptibility of Zirconium Containing Al-Zn-Mg Alloy Weld", Quarterly J. JWS, Vol. 4, No. 1 (1986) P. 120-125 (in Japanese)
24) S. Ohta, K. Asai and S. Ohya: "Study on Solidification of Aluminum Alloy Weld Metal (Report 1)", Trans. J. W. S., Vol. 16, No. 2 (1985) P. 35-46. (in Japanese)
25) S. Ohta, K. Asai and S. Ohya: "Investigation on Temperature Distribution and Cooling Rate in Molten Pool", Journal of the JWS, Vol. 8, No. 1 (1990) P. 59-65. (in Japanese)
26) S. Ohta, K. Asai and S. Ohya: "The Behavior of Temperature Decreasing and Fraction Solid Increasing in SoLid-Liquid Coexisting Zone", Journal of the JWS, Vol. 8, No. 2 (1990) P. 40-46. (in Japanese)
27) Japan Light Metal Association: "Aluminum Handbook", P. 22. (in Japanese)
28) T. Takahasi, T. Suzuki and K. Ichikawa: "Undecooling in Al-4wt%Cu Alloy", Journal of the JWS, Vol. 32, No. 5 (1968) P. 821-825. (in Japanese)
29) R. Ichikawa, T. Ohashi and T. Ikeda: "Supercooling in the Solidification of Al-Cr, Al-Mn and Al-Zr Binary Alloys", Journal of the JIM, Vol. 34, No. 9 (1970) P. 929-935. (in Japanese)
30) T. Ikeda and S. Nishi: "A Study on the Solidification Phenomenon of Al-Sn-Cu Alloy by Rapid Cooling", Journal of the JIM, Vol. 45, No. 8 (1981) P. 832-840. (in Japanese)
31) T. Ikeda and S. Nishi: "A Study on the Solidification Phenomenon of Al-Sn-Cu alloys by Rapid Cooling", J. JIM, Vol. 45, No. 8 (1981) P. 832-840 (in Japanese)